scientific reports

Check for updates

OPEN

Investigating screw-agitator speed ratio impact on feeding performance in pharmaceutical manufacturing using discrete element method

Luz Nadiezda Naranjo Gómez[1,3], Kensaku Matsunami[1], Paul Van Liedekerke[2], Thomas De Beer[3] & Ashish Kumar[1]✉

In continuous powder handling processes, precise and consistent feeding is crucial for ensuring the quality of the final product. The intermixing effect caused by agitators, which alters the powder's bulk density, flow rate, and flow patterns, plays a significant role in this process, yet it is often overlooked. This study combines discrete element method (DEM) modeling and experiments using a commercial-scale feeder to propose a Digital Twin (DT) framework. The DEM model accurately captures key flow features, such as bypass trajectories, stagnant zones, and preferential flow patterns, while providing quantitative predictions for the feed factor and zones prone to material accumulation. Scenario analysis is performed to identify the most favorable operating ranges of the screw-agitator ratio and screw speed, considering the cohesive properties of the powder. The study demonstrates that powders with poor flow characteristics require tighter operational constraints, as the screw-agitator ratio is susceptible to variations in mass feed rate. This contribution highlights the importance of selecting an appropriate screw-agitator ratio instead of maintaining a fixed value. Properly choosing this ratio helps determine an optimal operation window, which aims to achieve a minimum agitation level needed to induce unhindered flow and reduce variability in the mass flow rate.

Continuous manufacturing of solid dosage forms is essential to improve process flexibility and profitability while improving the end product quality[1]. Three main manufacturing routes from powder to tablets are: direct compression, dry granulation, and wet granulation. Irrespective of the selected route, feeding is a part of the unit operations as an initial or, in some cases, an intermediate step. Together with the blending unit, feeding is considered a critical step at which significant changes in formulation composition can be introduced, mitigated, or managed. Therefore, accurate and consistent feeding operation is crucial in determining the final formulation content, which influences the critical quality attributes of the end product.

In pharmaceutical production, twin-screw Loss-in-Weight (LIW) feeders are the preferred choice of equipment due to their reliable flow rates, even for difficult-to-handle powders. The system operates in gravimetric (controlled) and volumetric modes. It consists of a hopper for material storage, an agitator as a flow-aid, and a screw for convective transport. To secure a reliable and predictable flow, adequate compatibility between the design and operation of the gravimetric feeder and material properties is of central importance. This is to guarantee a smooth and continuous flow through the hopper and a consistent fill of screws in a uniform state of density. Nevertheless, obtaining an optimal feeder operation can be challenging due to the wide range of material's chemical and physical characteristics that have a role in the flowability of a material (i.e., particle size and shape, bulk density, compressibility, cohesive strength, and moisture, among others). Therefore, good flowing powders that tend to maintain a constant density typically pose few handling problems. On the other hand, when

[1]Pharmaceutical Engineering Research Group (PharmaEng), Department of Pharmaceutical Analysis, Ghent University, Ottergemsesteenweg 460, 9000 Ghent, Belgium. [2]Department of Data Analysis and Mathematical modeling, Ghent University, Coupure Links 653, 9000 Ghent, Belgium. [3]Laboratory of Pharmaceutical Process Analytical Technology (LPPAT), Department of Pharmaceutical Analysis, Ghent University, Ottergemsesteenweg 460, 9000 Ghent, Belgium. ✉email: ashish.kumar@ugent.be

handling more challenging materials that tend to stick in the hopper walls, bridge, or rathole, density conditioning, flow facilitation, and consistent screw filling are required, all of which can be achieved using an agitator.

The purpose of the agitation system is to act as a flow aid system that prevents bridging over the screws, disrupts stagnant regions, and sends material with a consistent density into the screw flights, promoting a stable and accurate mass flow rate. Despite its benefits, the agitator can also negatively impact the feeding process regarding material traceability due to its mixing effect and material accumulation in cases where the agitator aids powder compaction. The agitation is commonly performed using a mechanical stirrer close to the hopper's bottom, with a fixed rotational speed relative to the screw rotational speed. Its design generally varies depending on the hopper geometry in terms of orientation and blade shape. Recent literature studies have shown that the mixing behavior induced by the agitator is dependent on material properties and processing conditions[2,3]. This means that the screw-agitator ratio can directly influence the feeding behavior regarding flow patterns (e.g., funnel flow), bulk density distribution, mass flow rate variability, and changes in material traceability, among others. All these previously mentioned aspects suggest that it could be beneficial to independently control screw and agitator rotational speeds (i.e., not a fixed screw-agitator ratio). Studying this relevant and overlooked aspect of the feeding operation could lead to a better understanding of the feeding process. It could further help define an optimal operating region with less feeding variability, considering the material's characteristics.

Digital tools such as Digital Twin (DT) can offer a solution to provide a deeper understanding of the feeding process variations, promote innovation, and improve productivity, accelerating the time to market of medicines. The DT is generally defined as a digital informational construct of a physical system, created as an entity on its own and linked with the physical system[4]. It consists of a physical component, a virtual component, and automated data communication between these components. In this contribution, we focus on the virtual component, which considers the models used to simulate the physical process to assess the current and future state of the system. Within the virtual component commonly used models are data-driven based on multivariate predictions that require the collection of a large amount of experimental data[5–8], and more recently, computational models that use fundamental first principles to capture the underlying physical phenomena and predict the overall bulk behavior[9], such as finite element method (FEM), computational fluid dynamics (CFD), and discrete element method (DEM)[10]. Nevertheless, there is still a lack of a general model to predict such powder flow behavior for pharmaceutical applications.

This contribution focuses on one of the most commonly used mechanistic models for granular flow, DEM, which is used as a virtual component within the DT framework to represent the pharmaceutical feeding process and enable detailed simulation and analysis of powder flow dynamics within the equipment. In this numerical method, the macroscopic material behavior is predicted based on the dynamics of discrete particles. Therefore, the advantage of this modeling approach is that it offers a significant level of detailed insight into particle-level phenomena, which can sometimes be difficult or impossible to get experimentally. In addition, it enables the execution of parametric studies that consider the impact of changes in material properties, equipment design, and operating conditions. The model predictions provide insight into processes' operation, optimization, and troubleshooting, which can help speed up manufacturing process development. While DEM has been extensively used in several pharmaceutical applications[11], it remains underutilized in the prediction of powder flow and discharge in twin screw feeders. This is due to several reasons, such as the high computational time required to simulate particle dynamics in the micron size range, stringent process constraints, and the wide variability of powder and bulk properties[12,13]. Some of the strategies currently used to reduce computational time include: domain simplification, particle scale-up, time-step increment analysis, GPU computing, particle-level material tracking by extrapolation of DEM results[14], DEM-based reduced-order models[14], and multi-level coarse-graining technique[15,16].

The vast majority of DEM research available for screw feeders concentrates on the analysis of screw design and operating parameters effects on hopper drawdown patterns and flow rates using single screw systems with no agitator[11,17–19]. This makes it challenging to correlate the findings, as most of the feeders used in pharmaceutical applications are twin screws. On the other hand, more recent DEM studies like the one by Huang et al.[20] consider a twin-screw feeder with an agitated hopper. However, their analysis is limited to the feeding behavior of pellets, which cannot be directly extrapolated to the feeding behavior of pharmaceutical powders due to their unique material properties (e.g., cohesion). Up until now, there are only a limited number of DEM-focused articles that consider the complexity of the feeding system when considering both a twin screw agitated feeder and the properties of pharmaceutical powders[9,14,21]. Furthermore, to the author's knowledge, an experimental and DEM study considering the effect of the screw-agitator rotational speed ratio on the feeding performance of pharmaceutical powders is still missing. Due to this, this contribution aims to use a combination of experimental and predictive modeling approaches using DEM to understand and unveil the complex flow and mixing behavior induced by the agitator when changing the screw and agitator rotational speed ratio for pharmaceutical powders with different flowability levels. The insight could be considered a first step to assist in the adequate selection of feeding operating conditions based on the material's flow characteristics and a crucial step towards the integration of DT components in pharmaceutical manufacturing.

Materials and methods

This contribution uses a DEM predictive model to assess the effect of screw-agitator rotational speed on the feedability of powders with different flowability levels. For that purpose, a combination of experimental and DEM modeling approaches are used during model development steps: calibration, validation (i.e., emptying experiments), and feeding scenarios.

Materials

The materials used can be subdivided based on their particular application within the study. For the emptying experiments pink and white lactose-base free-flowing powder is used. For the emptying experiments, a binary blend of paracetamol powder (Mallinckrodt Chemical, Hazelwood, USA) and 10% sodium saccharine (JMC, South Korea) is used as a tracer material.

Equipment

A Brabender DDSR20-QR (Brabender Technologie GmbH & Co KG, Duisburg, Germany) twin-screw Loss In Weight (LIW) feeder equipment that enables independent control over screw and agitator rotational speed (i.e., separate drives) is used to study the effect of changes in the rotational speed ratios on powder feedability. The equipment consists of a bottom section of 2.5 L and a straight wall extension hopper of 5 L. In the conveying section, twin concave screws with a constant pitch of 20 mm are used. Above them, a vertical agitator with six blades is integrated to force powder flow from the hopper toward the screws to maintain a consistent screw flight filling. Besides, as shown in Fig. 1a, the equipment walls are selected to be partially (upper feeder section) or transparent, allowing for better visualization of the powder bed during the experiments.

For the feeding experimental trials, a customized test rig is mounted (Fig. 1b). It consists of the Brabender feeder with twin-concave screws, a conveyor belt below the feeder outlet, a SentroProbe Near Infrared (NIR) (Sentronic, Dresden, Germany) fixed above the conveyor belt, and a bin on top of a catch scale (Mettler Toledo, Zaventem, Belgium) at the end of the conveyor belt, to check the gain in mass with time.

Feeder characterization

The feeder is operated in volumetric mode (i.e., constant screw speed) to characterize the inherent feeding behavior of the considered materials for different operating conditions. The experimental volumetric runs are performed until the hopper is empty or unable to further deliver the remaining material in the hopper. Depending on the selected screw speed conditions and the material's inherent flow, the emptying duration varied. The obtained results in terms of change of mass of material per unit of time from either the catch scale (experiments) or virtual sensor (DEM model) are used to further calculate the feed factor (i.e., grams of material per screw revolution (g/rev)) as a function of time (s) or hopper fill level(%), using the following Eqs. 1, 2 and 3.

$$\text{Mass flow rate}\left(\frac{g}{s}\right) = \frac{\Delta m_{\text{catch scale}}(g)}{\Delta t(s)} \tag{1}$$

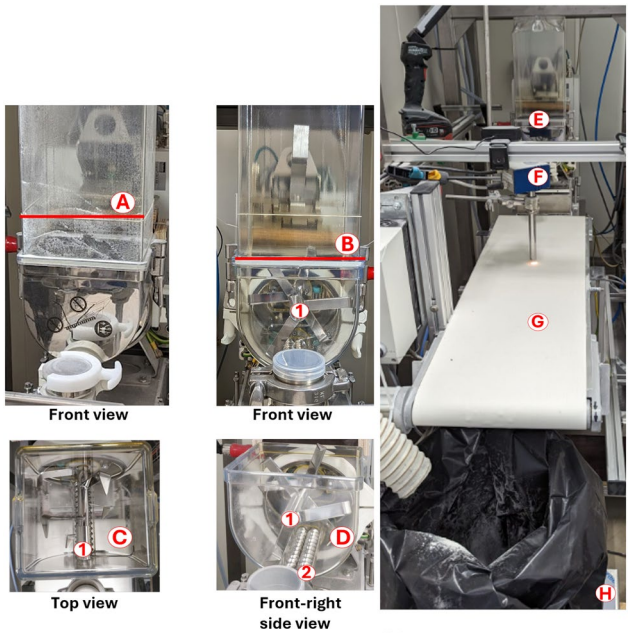

(a) LIW feeder system sections

(b) Customized feeder test rig sections

Fig. 1. Experimental setup for feeder emptying experiments with (**a**) LIW feeder system, red lines indicating powder transition levels for A: emptying experiments for paracetamol powder, B: emptying experiments for lactose-base powder, C,D: screw trough with an agitator (1) and concave screws (2). (**b**) Customized test rig used with sections, E: twin screw feeder, F: NIR probe, G: conveyor belt, and H: catch scale.

$$\text{Hopper fill level}(\%) = \frac{\text{Net weight}(g)}{\text{Max net weight}(g)} \times 100 \tag{2}$$

$$\text{Feed factor}\left(\frac{g}{rev}\right) = \frac{\text{Mass flow rate}\left(\frac{g}{s}\right)}{\text{Screw speed}\left(\frac{revolutions}{s}\right)} \tag{3}$$

Based on the feed factor profile, different descriptors can be derived, such as maximum feed factor, screw speed sensitivity, short-term feed factor variability, and feed factor decay. In this contribution, we focus on feed factor variability. Additional details regarding the feed factor profile descriptors can be found in Bekaert, Bram, et al.[5].

Discrete element method (DEM)

In DEM, the macroscopic material behavior is predicted based on the dynamics of discrete particles. Each particle is treated as a discrete element with a specific position and velocity, which is estimated for each time step based on the tangential and normal contact forces exerted on the particles. Newton's second law is solved numerically for each particle to track its motion in time[22]. The following equations are used to compute the rotational and translational motion (Eqs. 4 and 5). Here I, ω,M_p, t, υ, m,F_g, F_c, F_{nc}, and F_f are respectively the moment of inertia, angular velocity, contact torque, time, translational velocity, the mass of the particle, gravitational force, contact forces (e.g., elastic, plastic), non-contact forces (e.g., electrostatic, Van der Waals) and particle-fluid interaction forces (e.g., drag, pressure gradient)[22].

$$I\frac{d\vec{\omega}}{dt} = \vec{M_p} \tag{4}$$

$$m\frac{d\vec{\upsilon}}{dt} = \vec{F}_g + \vec{F}_c + \vec{F}_{nc} + \vec{F}_f \tag{5}$$

This study considers the commonly used soft-sphere discrete simulation approach. In this method, discrete particles are allowed to overlap to represent the deformation that occurs during collisions. The contact models use the amount of overlap between particles to calculate the magnitude of forces acting in normal and tangential directions. In pharmaceutical applications, selecting a contact model that considers the elastic properties of non-cohesive and cohesive materials is highly relevant to represent the interaction phenomena and overall bulk behavior adequately. Therefore, the commonly used Hertz–Mindlin contact model with Johnson–Kendall–Roberts (HM + JKR) is implemented in the model, which is frequently used for DEM modeling of pharmaceutical applications such as blending, fluid bed granulation, and twin-screw mixing[11,23].

The JKR is a non-linear elastic model that considers cohesion, allowing the representation of materials such as dry powders. In this model, the Johnson–Kendall–Roberts theory is used for the normal force estimation[24] and the Hertz–Mindlin contact model for the tangential force (limited by Coulomb friction $\mu_s F_c^n$), and the normal and tangential dissipation forces[25], as shown in the following Equations. Here the contact normal force F_c^n and contact normal dissipation force $F_c^{n,d}$ are estimated considering the values for equivalent Young's modulus E^*, equivalent radius R^*, contact radius a, surface energy γ for the first Eq. (6) and the values of relative coefficient of restitution β (restitution coefficient e), normal stiffness S_n, normal overlap δ_n, equivalent mass m^*, and normal component of the relative velocity υ_n^{rel} for Eq. (7).The maximum cohesion force, also called pull-out force $F_{pullout}$ is given by Eq. (9) and it is dependent on the critical contact overlap δ_c defined in Eq. (8). The contact tangential force F_c^t and the contact tangential dissipation force $F_c^{t,d}$ in Eqs. (12 and 13) are a function of the tangential stiffness S_t, tangential overlap δ_t, normal component of the relative velocity υ_n^{rel}, equivalent shear modulus G^*, and coefficient of static friction μ_s.

$$F_c^n = \frac{4E^*}{3R^*}a^3 - 4\sqrt{\pi\gamma E^*}a^{\frac{3}{2}} \tag{6}$$

$$F_c^{n,d} = -2\sqrt{\frac{5}{6}}\beta\sqrt{S_n m^*}\upsilon_n^{rel} \tag{7}$$

$$\delta_c = \frac{a_c^2}{R^*} - \sqrt{\frac{4\pi\gamma a_c}{E^*}} \tag{8}$$

$$F_{pullout} = -\frac{3}{2}\pi\gamma R^* \tag{9}$$

$$\beta = \frac{-ln\,e}{\sqrt{ln^2 e + \pi^2}} \tag{10}$$

$$S_n = 2E^* \sqrt{R^* \delta_n} \tag{11}$$

$$F_c^t = -S_t \delta_t \tag{12}$$

$$F_c^{t,d} = -2\sqrt{\frac{5}{6}} \beta \sqrt{S_t m^*} \upsilon_t^{rel} \tag{13}$$

$$S_t = 8G^* \sqrt{R^* \delta_n} \tag{14}$$

$$F_{compressive} = \sum F_c^n \tag{15}$$

The rolling resistance is accounted for by applying a torque to the contacting surfaces, considering the following equation with μ_r, R_i, and ω_i as the coefficient of rolling friction, the distance of the contact point from the center of mass, and the angular velocity vector at the contact point, respectively.

$$M_p = -\mu_r \mathrm{F_c^n R_i} \frac{\omega_\mathrm{i}}{\| \omega_\mathrm{i} \|} \tag{16}$$

To develop a predictive feeder model, the methodology shown in Fig. 2 is followed, which combines both experimental and modeling work in the initial and final steps. The steps include bulk calibration of DEM input parameters and model prediction validation. Subsequently, the DEM-validated model is used to predict the feeding behavior for a set of scenarios with changes in terms of material flowability and operating conditions (i.e., screw and agitator rotational speed).

Experimental work

Material calibration

The raw materials and blends are characterized following the procedures described by Van Snick, Bernd, et al.[26] for a subset of material descriptors. The descriptors are selected based on their potential use during DEM model calibration of input parameters. An overview of the selected descriptors and their considered relevance for the DEM input model parameters are mentioned in Table 1.

Feeder emptying experiments

Lactose-base free flowing colored powder

Before the start-up of the feeding operation, the feeder is tared. First, white lactose powder up to the level shown in Fig. 1a is manually filled in the empty feeder. Subsequently, the pink-colored powder is added on top of the

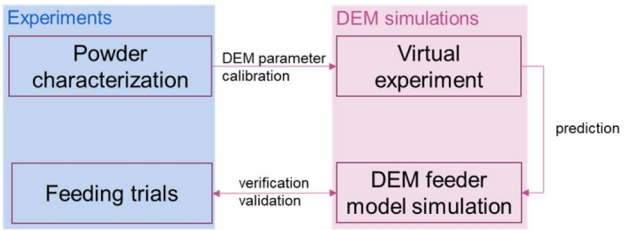

Fig. 2. DEM methodology steps followed combining experimental and modeling approaches.

Characterization method	Bulk property descriptor	Related DEM input parameters
Tapping device	Bulk and tapped density	
	Hausner ratio	
Granudrum*	Dynamic angle of repose	P–P** static friction
	cohesive index	P–P** rolling friction
FT4 powder rheometer	Flow rate index	Bulk density
	Flow energy (force and torque)	P–P/P–W** static friction
		JKR surface energy
		Coefficient of restitution

Table 1. Material characterization techniques used and their relation to DEM input parameters. *Granudrum: used only for the lactose-base free-flowing powder,**P–P: interaction between particles, P–W: interaction between particle and geometry wall.

white material powder bed present. Special attention is given to the gentle filling process to prevent powder densification and intermixing between layers.

Once the feeder filling process is completed, the feeder is set to run at a constant screw and agitator speed until it reaches almost empty conditions. The process is carried out for two extreme conditions in terms of the screw-agitator ratio of rotational speeds, considering a screw speed of 100 RPM and the screw-agitator ratios of 5 and 25. These experiments are performed to qualitatively validate the main model predictions regarding flow patterns in the feeding system.

Paracetamol powder

As performed during the emptying experiments with the lactose-base free flowing powder, the first experimental steps consist of taring, manually filling, and screw priming. In these cases, to perform the tracer step response experiments, the feeder is initially manually filled with paracetamol powder without any tracer in it up to the filled level shown in Fig. 1a and subsequently, the binary blend of paracetamol powder with 10% mass fraction of sodium saccharine is added on top up to a maximum hopper fill level.

After the filling process, the system is run in volumetric mode (i.e., at constant screw speed) until it is empty. During emptying, the powder going out of the feeder is transported by the conveyor belt, operating at a speed of 0.05 m/s, while the NIR spectra of the powder bed are collected. This spectra is later used to determine the chemical composition of the powder using a calibrated PLS chemometric model. Additional experimental details regarding the general procedure can be found in the paper by De Souter et al.[2]. At the end of the conveyor belt, a bin placed on top of a catch scale collects the powder. The actual mass flow values are estimated based on the gain in mass measured by the catch scale. This procedure is performed for two scenarios, considering a screw speed of 243 RPM (90% of feeder screw capacity, maximum screw speed = 270 rpm) and screw-agitator ratios of 15 and 25. The experimental results are further used during the validation of the predictive DEM model to gain additional insight into the feeding system when feeding a cohesive powder (i.e., paracetamol) in terms of feed factor values over time and visual identification of areas with material accumulation.

Model calibration and configuration

Model calibration

The model parameters used in this study are divided into two subtypes: intrinsic parameters and contact parameters. The intrinsic parameters, which depend on the material's properties, such as density, shear modulus, and Poisson's ratio, are fixed from literature values. The contact parameters, such as surface energy and static and rolling friction coefficients, are not established directly from experimental or literature values but are calibrated with virtual experiments. Therefore, the calibration procedure is performed to gain confidence in the model predictions by linking the material properties to the actual bulk behavior. The calibration methodology used in this study compares experimental tests carried out with the real material and the virtually replicated test. The DEM input parameters are adjusted to match the experimental bulk response with the predictions from the experiments. The calibration tests are selected to replicate the stress state and flow regimes expected in the real application case. Therefore, as low stresses and dynamic regime flow are expected in the agitated feeder, the most suitable calibration tests are considered to be the FT4 powder rheometer (Freeman Technology, Malvern, UK) and in the case of the lactose-base free flowing powder, also the rotating drum (GranuDrum, Granutools, Awans, Belgium).

The DEM input factors to be calibrated include rolling friction, static friction, and JKR surface energy. The results of the experimental bulk response and the virtual experiment prediction are compared in terms of dynamic flow angle and cumulative flow energy. The first test estimates flow ability and cohesion, and the second test is used to quantify powder resistance to flow (i.e., characterize powder flowability). Detailed information regarding the set of experiments and their results is outside the scope of this study. The methodology used is described in detail by Panteleev et al.[27] and Coetzee[28].

Based on the calibration results, the DEM input parameters are obtained. Table 2 shows the calibrated values for the lactose-base free-flowing powder. The selected set of parameters achieves a satisfactory representation of the behavior of the powder resistance to flow at different penetration depths in the FT4 rheometer and flow angles at different rotating speeds in a rotating drum, as seen in Fig. 3, with maximum relative errors of 8% and 4% respectively.

Model parameter	Value
Particle density (kg/m^3)	1530
Coefficient of restitution	0.5
Shear Modulus (Pa)	5×10^6
Poisson's ratio	0.25
Static friction P–P	0.6
Rolling friction P–P	0.1
Surface energy (J/m^2)	0.001, 0.35*

Table 2. DEM input parameters for lactose-base free-flowing powder. *Surface energy value for paracetamol powder.

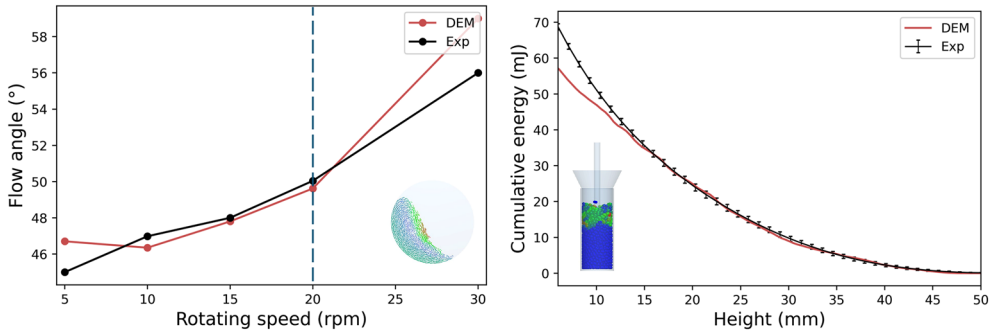

(a) Rotating drum **(b)** Powder rheometer

Fig. 3. Model calibration with FT4 rheometer with a blade tip speed of 100 mm/s and rotating drum for the lactose-base free-flowing powder. Comparison of experimental results and modeling predictions in terms of cumulative flow energy evolution with penetration depth and flow angle at different rotating speeds.

Based on the results shown in Fig. 3, it is possible to see that the selected set of input parameters can adequately capture the overall trend of both the cumulative energy and flow angle changes. However, the results show some discrepancies, such as the model's inability to predict the experimental results accurately. This is observed explicitly for the FT4 rheometer when the blade is located at the bottom of the cylindrical vessel when the accumulated flow energy is higher (heights lower than 10 mm in 3b) and for the rotating drum when the powder is at high rotational speeds (speeds higher than 20 rpm in 3a). The discrepancy between experimental values and model predictions could be partly caused by the differences in packing efficiency and mechanical interlocking of the larger particle size used in the model compared to the real particle size distribution.

DEM model configuration

The modeled system is the Brabender LIW twin screw feeder. The geometry consists of a hopper with two concave co-rotating screws located in a barrel and an integrated vertical agitator with counter-clockwise rotation. The feeder geometry in the model considers the exact dimensions as that of the equipment used to perform experiments (Fig. 4a).

The simulations are carried out using the DEM software Altair EDEM ®, 2022.2. The CAD model is imported using a high level of precision to avoid edge disturbances in the screw and agitator clearances, and the geometries are defined as physical rigid bodies with rotational dynamics added using linear rotation kinematics. The Hertz–Mindlin with JKR contact model is used as it takes into account two important aspects that dominate the mechanical behavior of particles in the feed system: elastic and adhesive interactions. Since different flowabilities are considered, the value of surface energy is modified accordingly to obtain the desired level of cohesivity. The DEM input values are selected based on the calibration approach for the specific representation of a particular powder. When exploring the effect of cohesion in the system (scenario analysis and case study sections), DEM input values are selected based on the typical median values representative of pharmaceutical powders.

To reduce model complexity, the particles are modeled as scaled monodispersed bi-spheres of 1 mm diameter, which is determined considering the maximum allowable size to avoid blockage artifacts in the system (i.e., particle size in comparison to the screw pitch clearances) while still reliably capturing the flow dynamics in the system.

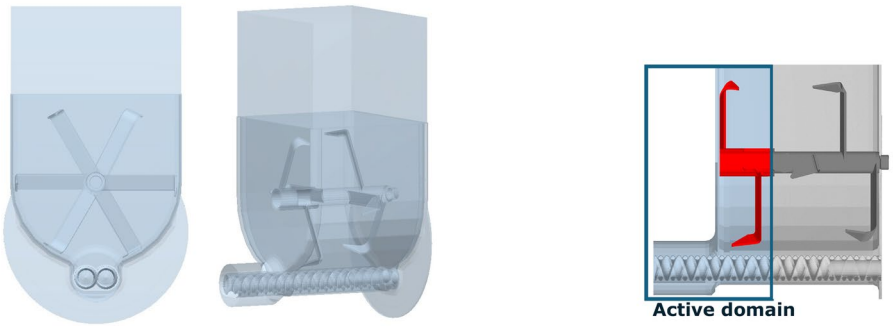

(a) Brabender feeder geometry **(b)** Simplified feeder geometry

Fig. 4. CAD model of LIW Brabender feeder with (**a**) side and front view and (**b**) simplified active feeder domain highlighted.

Mesh size and time step independence are verified to guarantee the computational efficiency and accuracy of the model results. A time step of 1.5×10^{-6} is selected as it is found not significantly to affect the simulation results.

Besides, a simplified virtual replica of the feeder with an initial medium fill level (i.e., hopper fill level around 50%) is used to reduce the computational cost of running full simulations with many particles in the feeder domain. This simplified system considers a wall to subdivide the entire domain, and to minimize the wall effects on flow profile development, the interaction coefficients are defined as those given for particle-particle interactions. The reduced domain (Fig. 4b) is numerically more efficient as the number of particles is considerably reduced (around 850,000 particles in the active domain), thus reducing the actual required computational time to run the simulation from start to end time (i.e., wall time), as seen in Table 3 while maintaining the same general flow behavior of the entire system.

The general computational procedure for each run consists of three steps. First, based on the calibrated or defined model input parameters, particles are generated within a geometry (i.e., particle factory) located above the agitator. Subsequently, the particles are allowed to fall and settle by gravity towards the bottom of the feeder. Lastly, the screw and agitation simultaneously start to mix and convey the particles towards the outlet of the feeder. The simulations are run for 60 s, with data being stored at intervals of 0.5 s to minimise the computational cost while capturing the main flow features (e.g., bypass pah, preferential extraction). The developed DEM feeder model is used to qualitatively and quantitatively assess the effect of operating conditions and flow properties changes on feeding performance. Additional information regarding the calibration process for different applications can be found in[29].

Model validation

The model results are qualitatively validated by performing a virtual replicate of the feeder emptying experiments for the lactose-base free flowing colored powder and comparing the simulated predictions with the previously obtained experimental results in a qualitative manner (i.e., image comparison) for the same cases experimentally studied. The comparison is made for flow profile development over time, and the identification of main flow features.

The sampling frequency of the physical experiments and simulations is not the same, and therefore, the average value of the experimental data obtained at two given hopper filling levels (i.e., medium and low) is calculated and used as a reference (green and red dotted sections in Fig. 6a) in the comparison with the simulation results. The levels represented by the red and green dotted sections in Fig. 6b,c indicate respectively the simulation's initial filling level and a low hopper level. The goal is to compare the feed factor values from both experiments and simulation when the process is at the same hopper filling level.

Subsequently, a validation case taking into account the feeder emptying experiments for paracetamol powder is performed, which is considered a challenging-to-feed powder due to its cohesivity. Two extreme cases with a screw speed of 243 RPM and a screw-agitator ratio of 15 and 25 are considered to analyze the agitator speed effect on the feeder performance. The simulation and experimental results are compared regarding feed factor values and the identification of zones prone to material accumulation. In the simulation, the predicted normal forces are used to identify zones prone to material accumulation since regions with higher normal forces indicate greater particle interaction and higher compressive forces.

In this case, to facilitate the analysis and identification of zones prone to material accumulation, two different regions are created in the system in the left and right bottom sections of the feeder, as seen in Fig. 7b, and the average value of normal force per region is estimated. A summary of the results considered during the validation process is shown in 4.

Scenario analysis

The validated DEM feeder model is used to predict feeding performance, considering a set of scenarios for each material (last row of Table 5) defined based on a three-level full factorial design of simulations. The parameters include powder screw-agitator ratio (3, 15, and 35) and screw rotational speeds (96, 170, and 243 RPM), as shown in the first two rows of Table 5.

The set of virtual emptying feeding experiments is performed for three powder flowability levels by changing the particle surface energy values in the DEM model (Table 5), going from free-flowing to cohesive, to unveil the effect of flowability on feeding performance. Results in terms of mass flow rate, flow patterns, variability of mass flow rate from setpoint, and average normal forces, among others, are obtained. A Projection to Latent Structure (PLS) regression is used to relate the input parameters (i.e., feeder operating conditions) to the output

Geometry representation	Required wall time (d)*
Full volume	100
1/2 volume	63
1/3 volume	55
1/3 volume**	15

Table 3. Computational time reduction from full to simplified domain with around 850,000 particles, considering a *wall time to obtain 5 minutes of simulation, using 4 NVIDIA A100-SXM4. The last column in the table is the time reduction obtained after time-step increment analysis (**).

Validation objective	Main results	Experiment	Virtual experiment
Qualitative: image analysis for feeder emptying Experiment: lactose-base free flowing colored powders (i.e, white, pink) Model: calibrated lactose-base free flowing powder with colored sub-layers	Main flow features: A:bypass path B:stagnant regions C:preferential extraction	Main flow features: A:pink-colored top powder layer dipped towards the bottom B:white powder stagnant in the bottom corner C:pink-colored top powder drawdown in the back	Main flow features: A:blue particle trajectory dipped towards the bottom B:unmixed colored sub-layers in the bottom corner C:uneven drawdown of colored powder sub-layers
Quantitative/Qualitative: mass flow rate values, image analysis for feeder emptying Experiment: paracetamol powder Model: calibrated paracetamol powder with colored sub-layers	D:feed factor values E:material accumulation	D:average feed factor values at the medium and low hopper fill levels E:images indicating zones with material accumulation	D:predicted feed factor values at the medium and low hopper fill levels E:time-averaged compressive forces per region

Table 4. Summary of the objectives for validation. The main results (second table column) are explained using experimental (third table column) and modeling methods (fourth table column).

Parameter	Values
Screw speed (RPM)	96, 170, 243
Screw-agitator ratio	3, 15, 35
JKR surface energy (J/m^2)	0.001–0.25

Table 5. Parameters and their values for the scenario analysis, DoS-virtual emptying experiments. A total of 9 scenarios considering as parameters screw speed and screw-agitator ratios (first two rows in the table) for each material (last row in table).

variables (i.e., the mean mass flow rate and deviations). The PLS uses the information obtained from the 9 DEM scenarios (3 level parameters: screw speed and screw-agitator ratio) for each material to predict the feeder's performance in unexplored operating regions, allowing the creation of contour plots for the different operating conditions and flowability levels. The procedure mentioned above serves as an example of a potential set of steps to consider to enhance the selection of operating ranges for better feeder performance using model predictions and process requirements.

Results and discussion

A detailed procedure is followed to develop a DEM model of a twin-screw feeder with calibrated parameters to predict the feeding behavior of powder. The global flow pattern predictions of the model are obtained and validated for aspects, such as the amount of material per screw revolution (feed factor) and normal forces. The validated model is subsequently used to assess the effect of changes in screw and agitator rotational speed on powders with different flowability levels, going from free-flowing to cohesive.

Validation using feeder emptying experiments

Lactose-base free flowing colored powder: main flow features

The DEM flow predictions allowed the visualization of the main flow features developed for a free-flowing lactose powder, considering a change in screw-agitator rotational ratio. Three general observations about the feeding process can be made based on the obtained flow profiles for both experimental and modeling approaches (Fig. 5a). First, there is a non-uniform flow profile where the agitator induces a bypass trajectory. The powder lying on top of the powder bed is dipped in by the agitator blades and is further forced to the bottom following the agitator trajectory. Thus, a portion of the powder at the top of the hopper leaves the system without thoroughly intermixing with other powder bed layers. The bypass path can be visualized in 5a, experimentally by the pink-colored powder trajectory going from the top layer towards the feeder outlet and in the predictions of the virtual experiment by following the position of the blue particle at each time step, starting from the left top layer going towards the feeder outlet. This finding agrees with the experimental observations by De Souter et al.[2] during their gravimetric tracer experiments and spatial sampling, where two flow zones are identified, bypass trajectory and inner mixing volume.

Second, as shown in Fig. 5b, there are stagnant zones in the feeder corners (i.e., white powder in feeder corners), which do not seem to be disturbed by the agitator during the emptying process. This is presumably caused by the agitator design. Throughout the emptying process, parts of the stagnant zones are disturbed by the agitator and intermixed with other layers. Nevertheless, part of the remaining unmixed stagnant powder does not leave the feeder.

Lastly, 5b shows that there is preferential extraction, where the powder drawdown mainly occurs at the back section of the feeder, leading to uneven flow in the front and back sections of the feeder. This is an expected behaviour due to the screw design used with a constant pitch. This can be seen both, experimentally and in the model by the pink-colored or top-layer powder at the back of the feeder, which flows preferentially faster towards the screws than the powder in the front region (red arrows in 5b).

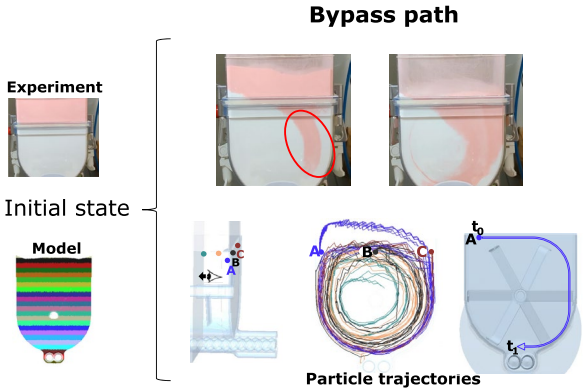

(a) Bypass visualization* (powder from top layer to bottom following agitator trajectory)

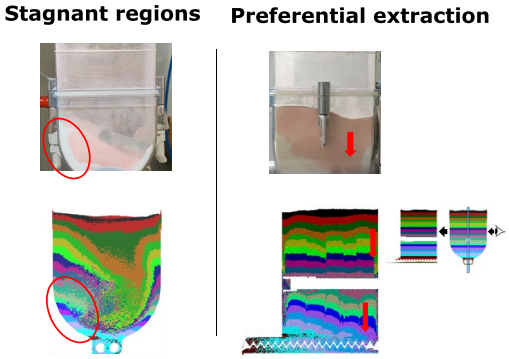

(b) Visualisation stagnant region (bottom corner) and preferential extraction (back drawdown)

Fig. 5. Validation considering experimental and modeling results. Main flow features: bypass path (pink-colored powder and blue particle A), stagnant regions (white, stagnant region bottom corner), and preferential extraction (red arrows, back drawdown). *Particle trajectories: trace particle positions at each time-step (blue particle A from t_0 to t_1).

Identifying all the previously mentioned behaviors is relevant as it directly influences the traceability of the materials in the system during batch-to-batch switching. Besides, it also highlights the effect and relevance of equipment design (e.g., agitator and screw design) on the development of flow patterns and possible flow challenges encountered in the system. It is crucial to know that the degree of influence and duration of the previously mentioned behaviors on the feeding process is directly dependent on the material properties of the powder to be fed as well as the operating conditions (i.e., screw-agitator rotational speed ratio). Therefore, feeder performance generalizations in terms of flow patterns for different powders cannot be made. Based on the qualitative similarities between the model and experiments, it can be confirmed that the developed DEM model can predict and capture the main flow features and can, therefore, be used as a starting point in the analysis of the effect of screw-agitator speed ratio.

Paracetamol powder: feed factor and material accumulation

A validation step for paracetamol powder is performed for two operational extreme conditions to gain additional confidence in the DEM model predictions. The obtained results allowed a quantitative comparison between experimental results and model predictions for feed factor values (i.e., the mass of material per screw revolution) and the identification of zones prone to material accumulation. As it can be seen in the feed factor plot, Fig. 6b,c, the DEM feeder model can adequately predict the mean experimental value used as a reference, giving a relative error of less than 7% considering the mean values of the simulation predictions of 1.23 g/rev and 1.08 g/rev for the cases with ratios 15 and 25 respectively at medium hopper level.

Regarding the identification of zones prone to material accumulation, it is evident from both experimental as well as model-based results shown in Fig. 7a that at the end of the emptying process, some powder tends to remain in a specific region of the feeder (i.e., left bottom). This zone is further identified in the model predictions before the emptied state by a regional comparison of normal forces (Fig. 7b), obtaining values up to 20 % higher for the average normal force in the left region compared to the right region.

Besides, based on the regional normal force comparison, it is observed that there are also differences between the two cases considered, with higher differences in average normal forces for the low screw-agitator rotational speed ratio (i.e., high agitator speed) compared to the case with a high ratio (i.e., low agitator speed), with values

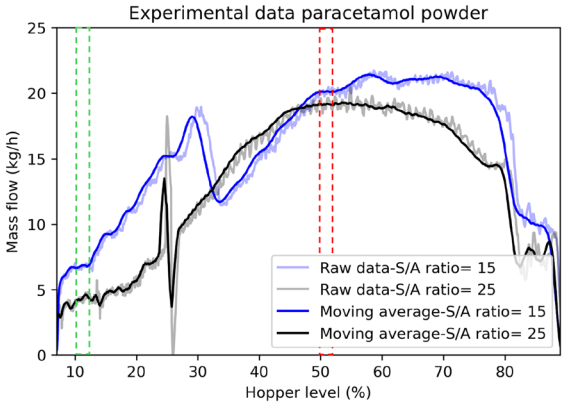

(a) Mass flow rate experimental values, paracetamol

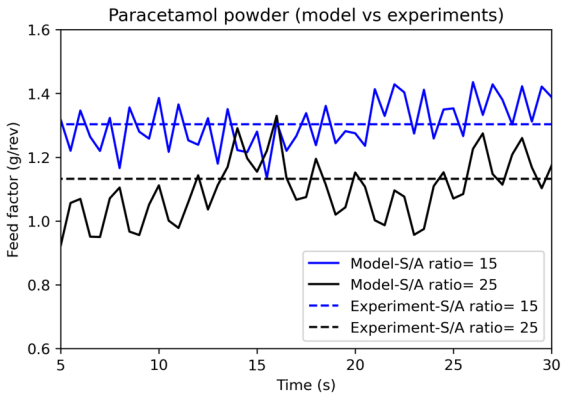

(b) Feed factor at medium hopper level

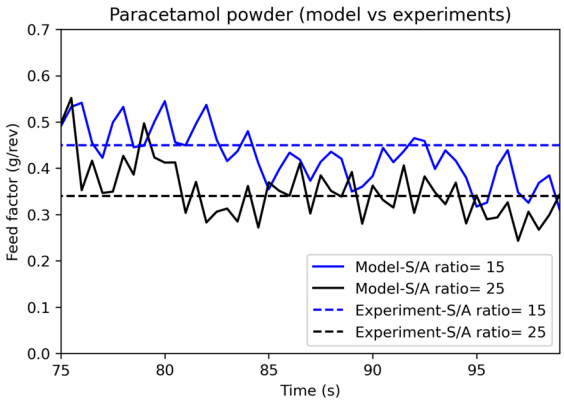

(c) Feed factor at low hopper level

Fig. 6. Experimental results of (**a**) mass flow rate values for different hopper levels. Red and green dotted lines indicate the values used to calculate the mean feed factor at medium and low fill levels, respectively. Feed factor comparison between experimental average feed factor value and model predictions for paracetamol powder at medium (**b**) and low (**c**) hopper fill level.

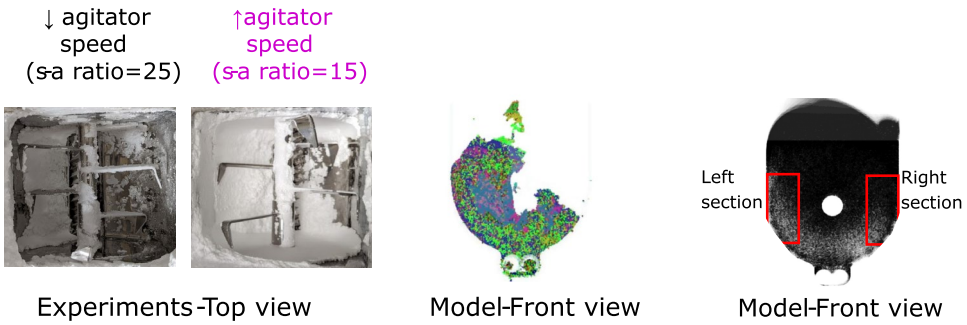

(a) Material accumulation

(b) Time averaged compressive forces

Fig. 7. Model and experimental results regarding material accumulation with (**a**) Material accumulation images (experiment and model predictions) and (**b**) time-averaged compressive forces (red boxes indicate regions considered for the calculation of average normal force).

of 20% compared to 4% respectively. This is in line with the experimental observations where higher piles of material are formed during the feeding process at higher agitator speeds compared to lower agitator speeds (Fig. 7a). This can be explained by the fact that the higher the rotation speed of the agitator, the greater the number of passes of the agitator blades through the powder bed per unit of time, which could, therefore, cause greater powder compression.

Scenario analysis

To gain a general process understanding regarding the effect of screw-agitator ratio on powder feedability, the validated DEM model is used as a tool to predict feeding performance when considering different process operating conditions: screw and agitator rotational speeds for powders with different flowability levels: free, intermediate, and poorly flowing (i.e., approximate flow function coefficients of 7, 3, and 1 respectively)[30].

DEM simulation results in terms of flow patterns and mass flow rate values are shown in Figs. 8 and 9. The screw-agitator ratio is observed to influence the obtained flow patterns in the system due to the mixing induced by the agitator, which in some cases can subsequently lead to variations in mass flow rate. This is especially evident for poorly flowing powders at a high screw-agitator ratio (i.e., low agitator speed), where the rotating agitator induces cyclic variations in the mass flow rate (Fig. 9b), which is dependent on the agitator blade positioning (see red blades in (Fig. 9b).

On the other hand, when considering free-flowing and intermediate powders, the DEM simulations show differences in the general flow patterns (Fig. 8) but little change in the mass flow rate obtained values when the screw-agitator relationship is modified, as seen in Fig. 9a. These observations for different powders could be explained by the fact that cohesive powders are expected to require additional mechanical aid to enable flow from the hopper to the screws when compared to free-flowing powders.

Based on the previous DEM simulation results for 9 data points (three-level full factorial design of simulations, Table 5, first two rows) for each material and interpolation based on PLS, the results are visualized using contour plots. This is to show the effect of feeder operation parameters (screw rotational speed and screw-agitator ratio) on the obtained mean mass flow rate and the standard deviation of the mass flow rate (Figs. 10 and 11). For free and intermediate flowing powders, as expected, mass flow rate values increase with higher values of screw speed. In both cases, there is a slightly higher mass flow rate variability at higher screw-agitator ratios (i.e., low agitator speed). Nevertheless, it is observed that the influence of changes in screw-agitator rotational speed cannot be considered significant in the mass flow rate standard deviation results (p-value<0.05), with p-values for free and intermediate flowing powders of 0.50 and 0.21, respectively. On the other hand, for poor flow powders, there is more significant variability of the mass flow rate for high screw-agitator ratios and, in this case, both the

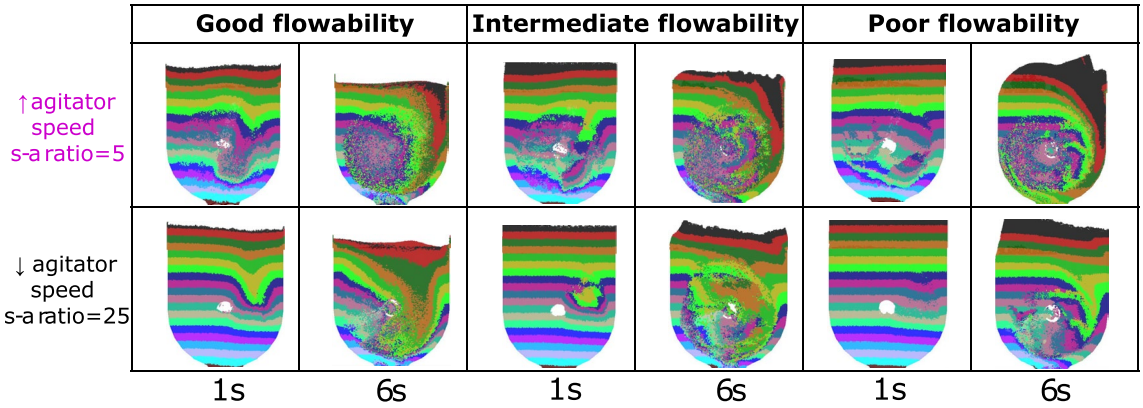

Fig. 8. Flow profiles for powders with different flowability levels (free, intermediate, and poorly flowing), considering a constant screw speed of 243 RPM and screw-agitator ratios of 15 and 25. Colored layers are used for visualization purposes only.

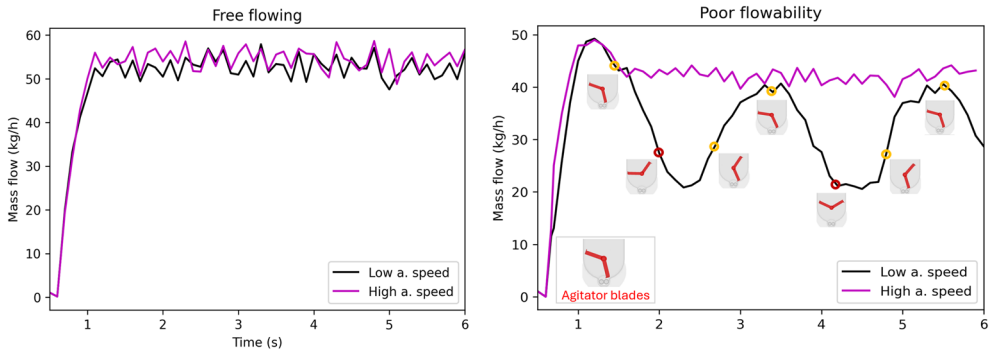

(a) Mass flow rate free- flowing powder

(b) Mass flow rate poorly flowable powder

Fig. 9. Mass flow rate values in time for (**a**) free and (**b**) poorly flowable powders, considering low and high agitator speeds (screw-agitator ratios of 15 and 25). Red blades to visualise their position in time.

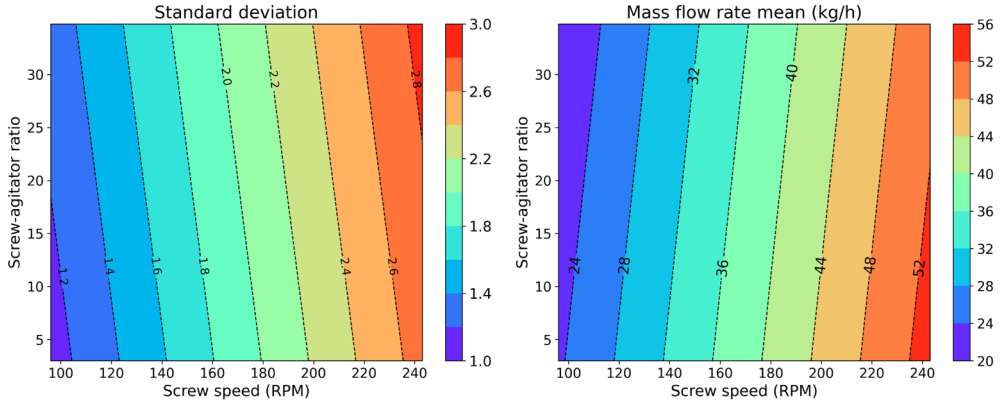

Fig. 10. Contours of mean mass flow rate and standard deviation values for a free-flowing powder. Results based on simulation results for 9 data points (three-level full factorial design of simulations and interpolation based on PLS).

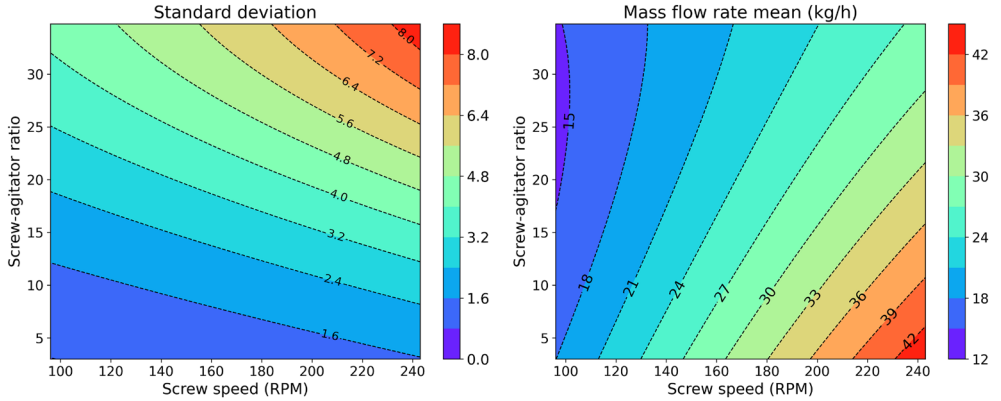

Fig. 11. Contours of mean mass flow rate and standard deviation values for a poorly flowable powder. Results based on simulation results for 9 data points (three-level full factorial design of simulations and interpolation based on PLS).

mean and the standard deviation are significantly influenced by both operational aspects (i.e., the screw ratio -agitator and screw speed), with p-values for screw-agitator ratio considering mean and mass flow rate standard deviation of 4.32×10^{-3} and 2.21×10^{-5}. In summary, considering the p-values, it can be said that the impact of the s-a ratio on the standard deviations of the mass flow rate is increasingly significant when moving from free powders to poor-flow powders. This highlights the relevance of appropriately choosing the operating conditions for these powders to reduce fluctuations in the feeding process.

Case study-identification of favorable operating range

Using the previously acquired contour plots, a model application case study is used to illustrate how to perform the determination of a suitable feeder operating condition. The contour plot of the mass flow rate mean is superimposed (i.e., overlaying one image over another) with that of standard deviation, in order to determine the most favorable operating range (i.e., pink area in contour plots) while also considering the mass flow rate requirements and the maximum allowable mass flow rate deviation.

In this case study, two requirements for mass flow rate between 25 and 30 kg/h and a maximum permissible variation of 2 kg/h are defined, and a favorable operating area (i.e., pink area) is obtained. Based on the favorable operating areas obtained (Fig. 12), it is confirmed that the currently used screw-agitator ratio equal to eight is within the favorable operating limits obtained for all cases considered.

Nevertheless, as can be seen in Fig. 12, when feeding free-flowing powders, as the screw-agitator ratio does not significantly influence the feeding process, more freedom in the selection of operating conditions is allowed (i.e., a larger favorable operating range) in comparison with the intermediate and poor flowing powders. The last one is the case with more operating restrictions and, therefore, a smaller area. Besides, based on the operating area, it can be concluded that higher agitator speeds (low screw: agitator ratios) are favorable for the feeding process of cohesive powders.

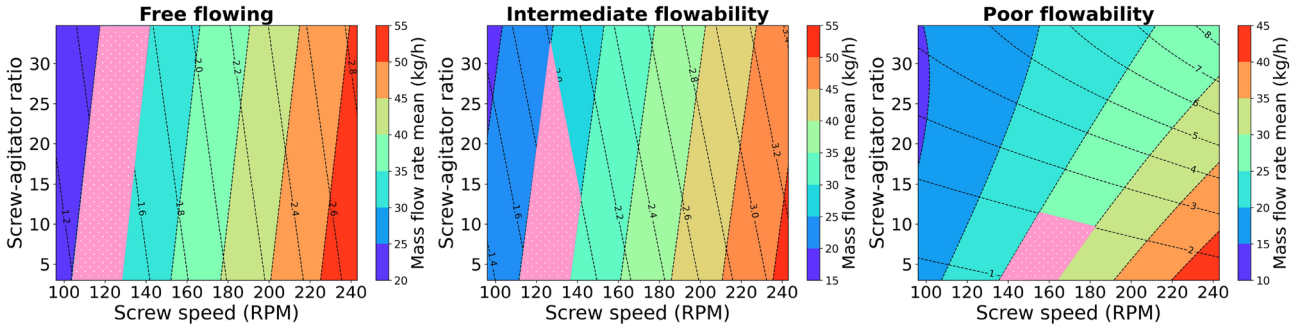

Fig. 12. Contours of the most favorable operating range (i.e., pink area) for powders with different flowability levels, considering changes in screw-agitator ratios and screw speed.

Therefore, based on the previously obtained results, it is clear that determining an optimal or adequate screw-agitator ratio is necessary for poorly flowing powders to guarantee a feeding operation that maintains a consistent mass flow rate. On the other hand, the findings help us exemplify how to improve the screw agitator feeding system for robust operation with powders with different flowabilities. In the current exemplified case study, a low screw-agitator ratio (i.e., less than 10) is recommended. This is because low values are within the favourable operating range obtained for all flowability levels considered (i.e. a pink area in 12 for free, intermediate, and poor flowable powders). However, when selecting an operational range, care must be taken to minimize the agitation required, as high agitation values (i.e., low screw-agitator ratios) could also increase energy consumption, particle attrition, and induced system vibrations.

Conclusions

In this paper, experimental and DEM predictive modeling approaches are used to analyze the effect of changes in the screw agitator ratio and screw speed on the feedability of pharmaceutical powders with different flowability levels. The DEM model differs from the current research available for twin screw feeders for two reasons. First, due to the approach used for model development, considering a quantitative and qualitatively validated DEM model capable of reliably capturing the dynamics of the agitated feeding system flow for pharmaceutical powders for various operating conditions and powder flowabilities while maintaining a reasonable computational cost due to the domain simplification and particle scaling. Secondly, due to the topic of analysis that considers a commonly overlooked effect: the changes in the rotation speed of the agitator on the intermixing impact and its relevance in the formation of powder accumulation regions. The results provide information on the appropriate selection of feeding operating conditions in terms of screw and agitator rotation speeds based on material flow characteristics.

The experimental results and model predictions allowed the visualization of three main flow features induced by the equipment design and affected by the feeding operation and material flow characteristics: non-uniform flow with a bypass trajectory, formation of stagnant zones in the feeder corners, and preferential back drawdown powder extraction. Besides, based on the results for paracetamol powder, it was possible to identify and experimentally validate the locations of zones prone to material accumulation near the corners of the hopper bottom. Lastly, it is shown that poorly flowing powders are more sensitive to changes in the agitator rotational speed in mass flow rate variability and, therefore, more operationally restricted when wanting to maintain a consistent and reliable mass flow rate. This is concluded considering the results of favorable operating ranges, with a range for the screw-agitator ratio between 5 and 30 for free-flowing powders and a more restricted range between 5 and 13 for cohesive powders.

This work demonstrated DEM's capabilities as a decision-support tool within the DT framework in determining suitable operating conditions and confirmed the relevance of an appropriate selection of the screw-agitator ratio in the feeding process. This framework could guarantee, in some cases (e.g., cohesive powders), a system less prone to feeding challenges with reduced mass flow rate variability. Furthermore, the results obtained could be considered as an initial step towards determining a suitable or optimal operating window (e.g., a minimum agitation level required to induce unimpeded flow or reduce mass flow variability from the set point) rather than keeping a fixed ratio.

While this research provides new insights into the relevance of the agitator's intermixing effect and adds yet another factor to consider when improving feeding operation performance (i.e., agitator speed), further research is required to investigate different equipment designs and a more comprehensive set of materials. All this is to extrapolate the system's knowledge to aid process control and equipment design and improve the development of compartmental models to trace the material in the continuous manufacturing lines.

Despite capturing the main flow characteristics, the model cannot provide insight into the microdynamics in regions with small clearances, such as screw-barrel and regions adjacent to the agitator blade tips. This is mainly attributed to the large DEM particle size used. Furthermore, due to the significant computational expense of running the model until empty conditions, some phenomena occurring during the later stages of the process, such as material pile formation, are not considered in the analysis and must be included in the future feeder performance analysis.

Data availability

The authors declare that the data supporting the findings of this study are available within the paper. Should any raw data files be needed in another format, they are available from the corresponding author upon reasonable request.

Received: 24 May 2024; Accepted: 5 September 2024
Published online: 11 September 2024

References

1. Nagy, Z. K., El Hagrasy, A. & Litster, J. *Continuous Pharmaceutical Processing* Vol. 42 (Springer, 2020).
2. De Souter, L. *et al.* Elucidation of the powder flow pattern in a twin-screw LIW-feeder for various refill regimes. *Int. J. Pharm.* **631**, 122534 (2023).
3. Waeytens, R. *et al.* An extended 3-compartment model for describing step change experiments in pharmaceutical twin-screw feeders at different refill regimes. *Int. J. Pharm.* **627**, 122154 (2022).
4. Grieves, M. & Vickers, J. Digital twin: Mitigating unpredictable, undesirable emergent behavior in complex systems. Transdisciplinary perspectives on complex systems: New findings and approaches 85–113 (2017).
5. Bekaert, B. *et al.* Determination of a quantitative relationship between material properties, process settings and screw feeding behavior via multivariate data-analysis. *Int. J. Pharm.* **602**, 120603 (2021).
6. Engisch, W. E. & Muzzio, F. J. Loss-in-weight feeding trials case study: Pharmaceutical formulation. *J. Pharm. Innov.* **10**, 56–75 (2015).
7. Cartwright, J. J., Robertson, J., D'Haene, D., Burke, M. D. & Hennenkamp, J. R. Twin screw wet granulation: Loss in weight feeding of a poorly flowing active pharmaceutical ingredient. *Powder Technol.* **238**, 116–121 (2013).
8. Van Snick, B. *et al.* Impact of material properties and process variables on the residence time distribution in twin screw feeding equipment. *Int. J. Pharm.* **556**, 200–216 (2019).
9. Bhalode, P. & Ierapetritou, M. Discrete element modeling for continuous powder feeding operation: Calibration and system analysis. *Int. J. Pharm.* **585**, 119427 (2020).
10. Pandey, P. & Bharadwaj, R. *Predictive Modeling of Pharmaceutical Unit Operations* (Woodhead Publishing, 2016).
11. Yeom, S. B. *et al.* Application of the discrete element method for manufacturing process simulation in the pharmaceutical industry. *Pharmaceutics* **11**, 414 (2019).
12. Ketterhagen, W. R., am Ende, M. T. & Hancock, B. C. Process modeling in the pharmaceutical industry using the discrete element method. *J. Pharm. Sci.* **98**, 442–470 (2009).
13. Sakai, M. How should the discrete element method be applied in industrial systems?: A review. *KONA Powder Part. J.* **33**, 169–178 (2016).
14. Toson, P. & Khinast, J. G. A dem model to evaluate refill strategies of a twin-screw feeder. *Int. J. Pharm.* **641**, 122915 (2023).
15. De, T. *et al.* A particle location based multi-level coarse-graining technique for discrete element method (dem) simulation. *Powder Technol.* **398**, 117058 (2022).
16. Mahto, L. *et al.* Accelerated dem simulation of the hopper-screw feeder and tablet-press feeder using the multi-level coarse-graining technique. *Powder Technol.* **436**, 119466 (2024).
17. Li, X., Hou, Q., Dong, K., Zou, R. & Yu, A. Promote cohesive solid flow in a screw feeder with new screw designs. *Powder Technol.* **361**, 248–257 (2020).
18. Hou, Q., Dong, K. & Yu, A. Dem. study of the flow of cohesive particles in a screw feeder. *Powder Technol.* **256**, 529–539 (2014).
19. Fernandez, J. W., Cleary, P. W., McBride, W. *et al.* Effect of screw design on hopper draw down by a horizontal screw feeder. in *Seventh International Conference on CFD in the Minerals and Process Industries CSIRO* 9–11 (Melbourne, Australia 2009).
20. Huang, T., Qian, H., Li, Z., Zuo, T. & Wu, B. Promoting pellet feed flow in a screw feeder with an agitator. *Ind. Eng. Chem. Res.* **62**, 6273–6284 (2023).
21. Bhalode, P. & Ierapetritou, M. Discrete element modeling (dem) parametric study of feeder unit in continuous pharmaceutical industry. in *Computer Aided Chemical Engineering*, vol. 47, 341–346 (Elsevier, 2019).
22. Naranjo, L., Nopens, I., De Beer, T. & Kumar, A. Effect of air dynamics on the discharge of a pharmaceutical powder using the discrete element method. in *Computer Aided Chemical Engineering*, vol. 51, 289–294 (Elsevier, 2022).
23. Behjani, M. A., Motlagh, Y. G., Bayly, A. E. & Hassanpour, A. Assessment of blending performance of pharmaceutical powder mixtures in a continuous mixer using discrete element method (dem). *Powder Technol* **366**, 73–81 (2020).
24. Johnson, K. L., Kendall, K. & Roberts, A. Surface energy and the contact of elastic solids. *Proc. R. Soc. Lond. A. Math. Phys. Sci.* **324**, 301–313 (1971).
25. Mindlin, R. D. & Deresiewicz, H. Elastic spheres in contact under varying oblique forces. *J. Appl. Mech.* **20**, 327–344. https://doi.org/10.1115/1.4010702 (2021).
26. Van Snick, B. *et al.* A multivariate raw material property database to facilitate drug product development and enable in-silico design of pharmaceutical dry powder processes. *Int. J. Pharm.* **549**, 415–435 (2018).
27. Pantaleev, S., Yordanova, S., Janda, A., Marigo, M. & Ooi, J. Y. An experimentally validated dem study of powder mixing in a paddle blade mixer. *Powder Technol.* **311**, 287–302 (2017).
28. Coetzee, C. J. Particle upscaling: Calibration and validation of the discrete element method. *Powder Technol.* **344**, 487–503 (2019).
29. Coetzee, C. Calibration of the discrete element method. *Powder Technol.* **310**, 104–142 (2017).
30. Schulze, D. *Powders and Bulk Solids* (Springer, 2021).

Acknowledgements

The computational resources and services used in this work were provided by the VSC (Flemish Supercomputer Center), funded by the Research Foundation Flanders (FWO) and the Flemish Government - department EWI. Financial support for this research from the BOF (Bijzonder Onderzoeksfonds Universiteit Gent, Research Fund Ghent University) and experimental support from Fette Compacting (Fette Compacting, Mechelen, Belgium) are gratefully acknowledged.

Author contributions

L.N.N.G conducted the experiments and simulations, analyzed the results, and prepared the manuscript. K.M. provided support in the methodology, analysis of results, and manuscript preparation. A.K., P.V.L., and T.D.B. contributed to the supervision, reviewing, and editing process. All authors reviewed the manuscript.

Competing interests
The authors declare no competing interests.

Additional information
Correspondence and requests for materials should be addressed to A.K.

Reprints and permissions information is available at www.nature.com/reprints.

Publisher's note Springer Nature remains neutral with regard to jurisdictional claims in published maps and institutional affiliations.